ELSEVIER

Computers and Chemical Engineering 27 (2003) 111–130

Computers & Chemical Engineering

www.elsevier.com/locate/compchemeng

Multiobjective optimization of an industrial styrene reactor

Amy K.Y. Yee, Ajay K. Ray, G.P. Rangaiah *

Department of Chemical and Environmental Engineering, National University of Singapore, 10 Kent Ridge Crescent, Singapore 119260, Singapore

Received 20 July 2001; received in revised form 16 May 2002; accepted 5 August 2002

Abstract

The paper describes a multiobjective optimization study for industrial styrene reactors using non-dominated sorting genetic algorithm (NSGA). Several two- and three- objective functions, namely, production, yield and selectivity of styrene, are considered for adiabatic as well as steam-injected styrene reactors. Pareto optimal (a set of equally good) solutions are obtained due to conflicting effect of either ethyl benzene feed temperature or flow rate. The results provide extensive range of optimal operating conditions, from which a suitable operating point can be selected based on the specific requirements in the plant.

Keywords: Simulation; Multiobjective optimization; Styrene reactor; Genetic algorithm; Pareto sets

1. Introduction

Styrene is one of the most important monomers produced worldwide, and finds major use in the production of polystyrene, acrylonitrile–butadiene–styrene resins (ABS), and a variety of miscellaneous polymers in the petrochemical industry (Li & Hubbell, 1982; Chen, 1992; Denis & Castor, 1992). In US, it ranks fourth in the most manufactured monomer behind ethylene, vinyl chloride and propylene (Chen, 1992). Styrene is produced commercially by catalytic dehydrogenation of ethyl benzene, and the average plant capacity is over 100 000 tons per year. Therefore, the investment cost is very high, and even a small improvement in the plant operation can generate significant revenue. Hence, optimal design and operation of the styrene reactor are required, as it is the critical equipment in styrene manufacturing process.

Many studies on kinetics, reactor modeling, simulation and optimization of the styrene reactor have been reported. More than 50 years ago, Wenner and Dybdal (1948) obtained rate data from experiments for two types of catalysts. Sheel and Crowe (1969) determined rate coefficients and heat of reactions from the industrial data of an adiabatic styrene reactor using a pseudo-homogeneous model. Sheppard, Maier and Caram, (1986) obtained the best kinetic model by calibrating several models using catalyst manufacturers' data. Of these models, the kinetic model proposed by Sheel and Crowe (1969) has been widely used (Clough & Ramirez, 1976; Elnashaie, Abdalla & Hughes, 1993; Abdalla, Elnashaie, Alkhowaiter & Elshishini, 1994; Savoretti, Borio, Bucalá & Porras, 1999). Pseudo-homogeneous model had been used by most researchers for simulation and optimization of industrial reactors (Sheel & Crowe, 1969; Clough & Ramirez, 1976; Sheppard et al., 1986; Elnashaie & Elshishini, 1994; Savoretti et al., 1999). Elnashaie et al. (1993) developed a rigorous heterogeneous model based on dusty gas model. They used the model to extract intrinsic kinetic data from industrial data iteratively. In another paper, Abdalla et al. (1994) reported intrinsic kinetics for three promoted iron oxide catalysts using the pseudo-homogeneous and heterogeneous model, and compared the performance of these catalysts.

There had been several studies on optimization of the styrene reactor but involving single objective function only. Sheel and Crowe (1969), Clough and Ramirez (1976) performed multivariable optimization on both adiabatic and steam-injected reactor to maximize a profit function. For adiabatic reactor, the former study selected steam temperature, steam flow rate and reactor length as the decision variables whereas Clough and

* Corresponding author. Tel.: +65-6874-2187; fax: +65-6779-1936
E-mail address: chegpr@nus.edu.sg (G.P. Rangaiah).

0098-1354/02/$ - see front matter
PII: S0098-1354(02)00163-1

Nomenclature

A	frequency factor (−); cross-sectional area of reactor (m^2)
C	molar concentration ($kmol/m^3$)
Cp	molar heat capacity (kJ/kmol per K)
D	diameter (m)
E	activation energy (kJ/kmol)
F	molar flow rate (kmol/h)
G	mass velocity of the gas mixture (kg/m^2 per h)
H	cost factor ($/kmol)
k	reaction rate constant (kmol/kg per h per bar^n)
K	equilibrium rate constant (bar)
L	total length of the reactor (m)
N	number (−)
p	partial pressure (bar); probability (−)
P	total pressure (bar)
R	universal gas constant (8.314 kJ/kmol per K)
r	reaction rate (kmol/kg per h)
S	selectivity (%)
SOR	steam over reactant (ethyl benzene) molar ratio (−)
T	temperature (K)
X	conversion (%)
Y	yield (%)
Z	length of the reactor (m)
Greek symbols	
ε	void fraction (−)
ρ	density (kg/m^3)
μ	viscosity (kg/m per s)
ΔH	heat of reaction (kJ/kmol)
λ	fraction of reactor bed where steam is injected (−)
δ	fraction of steam distributed (−)
Subscripts/superscripts	
o	initial
b	bulk
bz	benzene
c	cross-over
C	catalyst
CO	carbon monoxide
CO_2	carbon dioxide
eb	ethyl benzene
eth	ethylene
G	gas
gen	generation
H_2	hydrogen
i	reaction i
j	component j
m	mutation
meth	methane
p	particle
st	styrene
steam	steam
t	total
tol	toluene

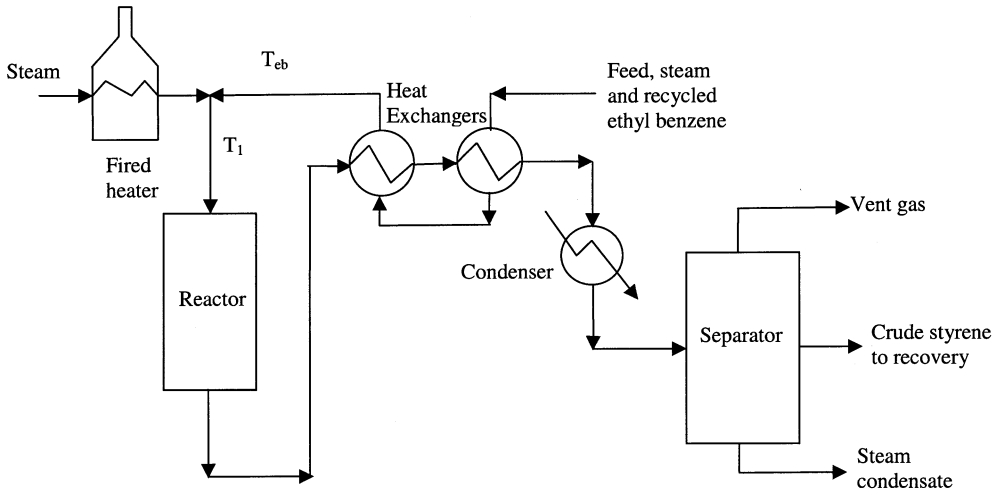

Fig. 1. Schematic diagram of catalytic dehydrogenation of ethyl benzene.

Ramirez (1976) chose steam to ethyl benzene ratio, ethyl benzene pre-heater exit temperature and steam temperature. For the steam injection case, steam was split into two fractions with one part introduced at the inlet of the reactor and the other part introduced at a particular location of the bed. Both the fraction and the location where the remaining part was introduced were the two additional decision variables in the studies of Sheel and Crowe (1969), Clough and Ramirez (1976). Results of both these studies indicated that there was improvement in performance when steam was divided into two fractions and injected along the reactor length in addition to the reactor inlet. Subsequently, Clough and Ramirez (1976) built a pilot plant and verified this improvement.

Sheppard et al. (1986) employed optimization to evaluate two types of catalysts: one with a higher selectivity and another with a higher activity. They chose profit function as the objective function and two decision variables, namely, steam to ethyl benzene ratio and steam inlet temperature, for both adiabatic and steam-injected reactor. Their study showed that economics for the catalyst with a high selectivity were better than those for the catalyst with a high activity. Sundaram, Sardina, Fernandez-Baujin and Hildreth, (1991) developed a simulator with optimization software incorporated in it for the entire styrene plant. Complex method of Box (1965) was employed to perform the optimization with all plant constraints.

Most real world problems involve the simultaneous optimization of multiple objectives. Solution and results of these problems are conceptually different from single objective function problems. In multiobjective optimization, there may not exist a solution that is the best with respect to all objectives. Instead, there could exist an entire set of optimal solutions that are equally good, which are known as Pareto-optimal solutions. A Pareto-optimal set of solutions is such that when we go from any one point to another in the set, at least one objective function improves and at least one other worsens. A recent review on the applications of multiobjective optimization in chemical engineering (Bhaskar, Gupta & Ray, 2000) reported several interesting studies on the multiobjective optimization of chemical reactors and processes. Early studies used the parametric method or the ε-constraint method to obtain the Pareto-optimal set of non-dominant solutions. More recently, our group has carried out multiobjective optimization studies on steam reformers (Rajesh, Gupta, Rangaiah & Ray, 2000) and hydrogen plant (Rajesh, Gupta, Rangaiah & Ray, 2001) using Non-dominated Sorting Genetic Algorithm (NSGA) (Srinivas & Deb, 1995). In the present work, two and three objective optimizations were carried out to obtain optimal operating conditions for both adiabatic and steam-injected styrene reactors. Suitable kinetic and reactor models were selected from the open literature for successfully simulating an industrial styrene reactor, and then multiobjective optimization was carried out using NSGA. To the best of our knowledge, this is the first attempt to study multiobjective optimization of an industrial styrene reactor, and provides a broad range of quantitative results useful for understanding and optimizing industrial styrene production.

2. Process description

Fig. 1 shows the simplified flow diagram for the production of styrene by dehydrogenation of ethyl benzene (Li & Hubbell, 1982; Chen, 1992; Denis & Castor, 1992). Fresh ethyl benzene mixed with recycled ethyl benzene and steam, is preheated using the product stream from the reactor, and then mixed with the

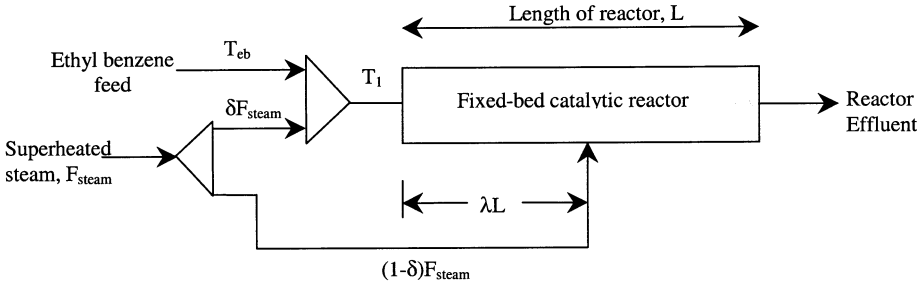

Fig. 2. Two-bed styrene reactor with steam injection partway of the reactor length.

superheated steam to reactor inlet temperature of over 875 K before injecting into the fixed bed catalytic reactor. Superheated steam provides the necessary heat of reaction, inhibits coke formation and reduces the partial pressure of styrene and hydrogen to shift the thermodynamic equilibrium in favor of the styrene production. Molar ratio of steam to ethyl benzene in the feed entering the reactor is usually 15. The reactor effluent is cooled to quench all reactions in several heat exchangers, and then directed to the separator to recover styrene.

Six main reactions occurring in the styrene reactor are:

$$C_6H_5CH_2CH_3 \rightleftharpoons C_6H_5CHCH_2 + H_2 \quad (1)$$

$$C_6H_5CH_2CH_3 \rightarrow C_6H_6 + C_2H_4 \quad (2)$$

$$C_6H_5CH_2CH_3 + H_2 \rightarrow C_6H_5CH_3 + CH_4 \quad (3)$$

$$2H_2O + C_2H_4 \rightarrow 2CO + 4H_2 \quad (4)$$

$$H_2O + CH_4 \rightarrow CO + 3H_2 \quad (5)$$

$$H_2O + CO \rightarrow CO_2 + H_2 \quad (6)$$

Dehydrogenation of ethyl benzene, $C_6H_5CH_2CH_3$ (Eq. (1)) is an endothermic reversible reaction, and proceeds with low yield thermally but with high yield catalytically. As it is an endothermic reaction producing two moles of product to one mole of reactant, low pressure and high temperature favor forward reaction producing styrene, $C_6H_5CHCH_2$. At equilibrium, the reversible reaction (Eq. (1)) results in about 80% conversion of ethyl benzene. However, the time and temperature necessary to achieve this give rise to excessive thermal cracking. The competing thermal reactions (Eqs. (2) and (3)) degrade ethyl benzene to by-products such as benzene (C_6H_6) and toluene ($C_6H_5CH_3$), and thus reduce styrene yield. As the rate of formation of by-products increases with temperature, an optimal operating temperature is necessary to compromise between conversion of ethyl benzene to styrene and by-product formation. In addition, a selective catalyst is desirable to achieve high styrene yield at low temperature and to minimize side reactions.

3. Reactor model and simulation

For simulating an industrial styrene reactor, Sheel and Crowe (1969) employed a model assuming a plug flow reactor, and heat and mass transfer to as well as diffusion in the catalyst pellet were lumped in the rate constants. Thus, the model is a pseudo-homogeneous model. Later, Abdalla et al. (1994) and Elnashaie and Elshishini (1994) used this model as well as a more detailed heterogeneous model, which takes into account diffusion in the catalyst pellet. Predictions by both the models are comparable. For selecting one of these models for optimization, we tried both of them for simulating the industrial adiabatic reactor, whose design and operating conditions were reported by Sheel and Crowe (1969). Catalyst activity is considered constant due to lack of available data, even though it varies with both time and reactor length. Governing equations for the pseudo-homogeneous model as well as design and operating conditions of the reactor are summarized in Appendix A. All kinetic and property data are taken from Elnashaie and Elshishini (1994).

The model equations for both pseudo-homogeneous and heterogeneous models were solved on CRAY J916 supercomputer using IVPRK and NEQNF subprograms of the IMSL library for solving ordinary differential and nonlinear algebraic equations, respectively. The IVPRK subprogram is based on 5th and 6th order methods of Runge–Kutta–Verner for solving ordinary differential equations, with automatic selection of step size to ensure accuracy. Both reactor models gave results comparable to the industrial data as well as to those reported by Elnashaie and Elshishini (1994). The results for pseudo-homogeneous model are shown in Table A3. Computational time for simulating the industrial reactor by pseudo-homogeneous and heterogeneous models is, respectively, 0.062 and 1.1 s. Considering the good accuracy and significantly smaller computational time for one simulation by the pseudo-homogeneous model, this model is chosen for the multiobjective optimization study.

4. Multiobjective optimization

This study considers optimization of an existing reactor in a styrene plant. In such a case, reactor dimensions, available steam temperature and catalyst data are generally fixed. Two reactor configurations are considered for multiobjective optimization. The first is an adiabatic reactor in which the entire steam enters the reactor along with ethyl benzene stream at the inlet. In the second reactor configuration (Fig. 2), a fraction (δ) of steam is mixed with ethyl benzene at the reactor inlet while the remaining steam is injected at a certain point along the reactor, say, at λ fraction of the total reactor length. Thus for the adiabatic reactor, δ is equal to 1 and λ ($\equiv 0$) is not required.

Apart from the profitability as was used by earlier investigators, other possible objectives for optimizing a styrene reactor are the amount of styrene produced (F_{st}), selectivity of styrene (S_{st}) and the yield of styrene (Y_{st}).

$$\text{Maximize} \quad J_1 = F_{st} \tag{7}$$

$$\text{Maximize} \quad J_2 = S_{st} = \frac{F_{st} - F_{st}^{o}}{F_{eb}^{o} - F_{eb}} \tag{8}$$

$$\text{Maximize} \quad J_3 = Y_{st} = \frac{F_{st} - F_{st}^{o}}{F_{eb}^{o}} \tag{9}$$

Since profitability is strongly correlated with F_{st} and cost data vary from plant to plant and from time to time, we have considered combinations of only Y_{st}, S_{st} and F_{st} for two- and three-objective optimization.

For optimizing the operation of an adiabatic reactor, four decision variables are available. These and their bounds are:

$$550 < T_{eb} < 800 \ \text{K} \tag{10}$$

$$1 < P < 2.63 \ \text{bar} \tag{11}$$

$$7 < \text{SOR} < 20 \tag{12}$$

$$27.56 < F_{eb}^{o} < 40.56 \ \text{kmol/h} \tag{13}$$

The lower bound on ethyl benzene feed temperature (T_{eb}) is chosen as 550 K to ensure that the temperature of ethyl benzene and steam mixture at the reactor inlet, T_1 (Fig. 2) is not too low for the reaction to occur. The upper bound on T_{eb} is set at 800 K to prevent undesirable side reactions before ethyl benzene enters the reactor (Clough & Ramirez, 1976). The range for the inlet pressure, P is chosen based on the pressure at which industrial styrene reactors usually operate. The lower limit of the steam to ethyl benzene molar ratio, SOR (steam over reactant), is set at 7 to prevent coke formation on the catalyst surface and to remove coke deposits from the catalyst surface thereby regenerating it. However, if SOR is increased to a very high value, it will affect the economics of the process as extra energy is required to produce the excess steam and its subsequent condensation at the downstream of the reactor. Hence, it is usual industrial practice to restrict SOR at 20. The lower and upper bounds for the initial ethyl benzene flow rate, F_{eb}^{o} are taken to be -25 and $+10\%$ of the nominal value (36.87 kmol/h). These bounds are consistent with industrial practice since a plant can often be operated at a much lower capacity but not at a much higher capacity.

In addition to the above four decision variables, two additional variables (δ, fraction of steam used at the reactor inlet and λ, location of the injection port for the remaining steam expressed as a fraction of the total reactor length) can also be selected for optimizing steam-injected reactor.

$$0.1 < \delta < 1 \tag{14}$$

$$0.1 < \lambda < 1 \tag{15}$$

The lower bound is set at 0.1 instead of 0 to reduce the search space and thus facilitate optimization. The results presented later show that optimal δ and λ are above the lower limit, and practically the same results were obtained even with the lower limit of 0. It may or may not be possible to change λ in an existing reactor. However, this is also considered as the decision variable in order to consider a more general optimization problem.

The optimization is subject to three other constraints:

$$F_{steam} < 454 \ \text{kmol/h} \tag{16}$$

$$850 < T_1 < 925 \ \text{K} \tag{17}$$

$$850 < T_2 < 925 \ \text{K} \tag{18}$$

The constraint on the total steam rate, F_{steam} is based on the size-limitation of the downstream condenser as even though the furnace can produce more steam at a lower temperature, the product condenser may not be able to handle the increased throughput (Sheel & Crowe, 1969). Note that T_1 is the temperature of the ethyl benzene and steam mixture entering the reactor inlet (Fig. 2) and T_2 is the temperature at $z = \lambda L$. The constraints on the temperatures (Eqs. (17) and (18)) are based on the minimum temperature required for reaction to take place and the temperature at which catalyst starts to deactivate (Clough & Ramirez, 1976). Only Eqs. (16) and (17) are applicable for adiabatic reactor. All the three equations are for steam-injected reactor.

Optimization programs used in this work are for minimization of objective functions without constraints (other than bounds on decision variables). Maximization of a function (J) can be converted to a minimization problem by using the transformation of $I = 1/(1+J)$ or $I = [1/J]$ if $J \neq 0$. The constraints in Eqs. (16)–(18) are incorporated into each of the objective functions (Eqs. (7)–(9)) using penalty functions. The modified objective functions are:

$$I_1 = \frac{1}{F_{st}} + 10^4 \sum_{i=1}^{5} f_i \tag{19}$$

Table 1
Values of NSGA parameters used in this work

Number of generations, N_{gen}	100
Population size, N_{pop}	50
Sub-string length coding for each decision variable, l	32
Crossover probability, p_c	0.7[a]
Mutation probability, p_m	0.002
Maximum niche count distance, σ	0.05[a]
Exponent in sharing function, α	2.0
Seed for random number generator, S_r	0.75

[a] In case 3, $p_c = 0.5$, $\sigma = 0.7$.

$$I_2 = \frac{1}{S_{st}} + 10^4 \sum_{i=1}^{5} f_i \quad (20)$$

$$I_3 = \frac{1}{Y_{st}} + 10^4 \sum_{i=1}^{5} f_i \quad (21)$$

where

$$f_1 = (F_{steam} - 454) + |(F_{steam} - 454)| \quad (22)$$
$$f_2 = (850 - T_1) + |(850 - T_1)| \quad (23)$$
$$f_3 = (T_1 - 925) + |(T_1 - 925)| \quad (24)$$
$$f_4 = (850 - T_2) + |(850 - T_2)| \quad (25)$$
$$f_5 = (T_2 - 925) + |(T_2 - 925)| \quad (26)$$

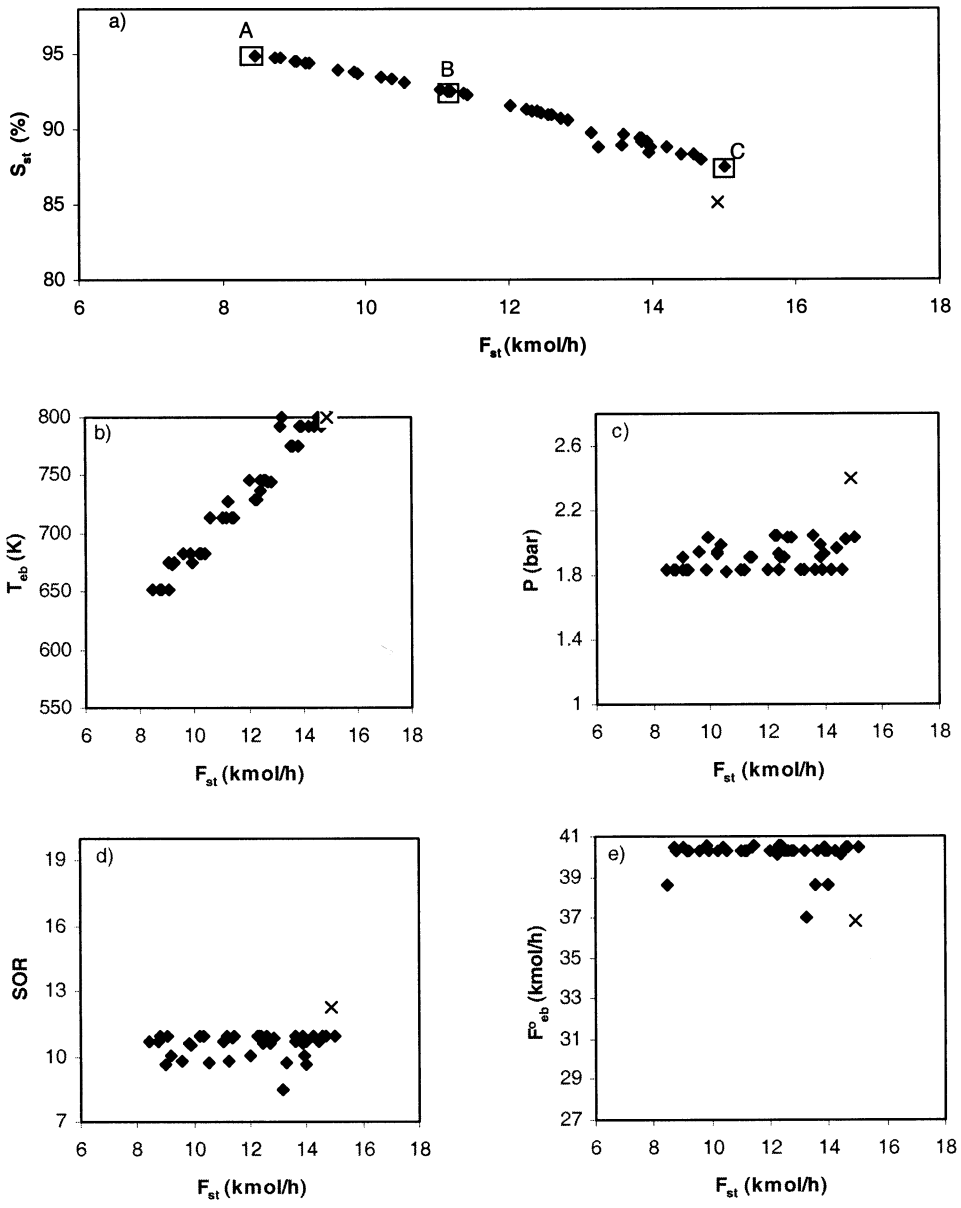

Fig. 3. Results for two-objective optimization (Case 1, maximization of F_{st} and S_{st}). (a) Pareto set; and (b–e) values of decision variables corresponding to the points shown in (a), × indicates industrial operating point.

Decision variables and their bounds are those shown in Eqs. (10)–(15). The resulting optimization problems are solved using an adapted version of genetic algorithm, referred to as NSGA for multiobjective optimization. Genetic algorithms and NSGA are briefly described in Appendix B. Further details on NSGA are available elsewhere (Srinivas & Deb, 1995; Bhaskar et al., 2000). Table 1 shows the values of NSGA parameters used to obtain the solutions. In the present study, several different values of these parameters were tried and best values were then chosen based on smoothness and spread of the Pareto optimal solution. These parameters are problem specific and should be selected properly for a particular problem. It was found that a slightly different set of NSGA parameters must be chosen for case 3.

5. Results and discussion

Optimization of the industrial styrene reactor is studied for the design and operating conditions given in Table A2 except for the inlet temperature (T_1), namely, 922.59 K which refers to the temperature of the ethyl benzene and steam mixture. For optimization, both T_{eb} and SOR are the decision variables, and hence temperature of the superheated steam is fixed at 1025 K (Clough & Ramirez, 1976) and T_1 is calculated by energy balance for the chosen values of T_{eb}, SOR and δ. This calculation takes into account some steam (50.4 kmol/h) at T_{eb} in the ethyl benzene feed, consistent with industrial practice in order to avoid undesirable reactions prior to the reactor. Note that SOR includes this amount also. An optimization problem that involves two or more objective functions often give rise to Pareto set when decision variables act in conflicting manner. A Pareto set is such that when one moves from one point to another on the Pareto, at least one objective improves while at least one other objective worsens. Hence, neither of the solutions dominates over each other, and all solutions on the Pareto are equally good. One has to use additional information to choose an operating point from among the entire set of equally good optimal solution for efficient operation. This point is usually determined by engineer's experience and requirement, and is often site specific.

6. Two-objective optimization

Three cases of two-objective optimization are possible for the three objectives, namely, maximization of F_{st}, S_{st} and Y_{st} (Eqs. (7)–(9)). Results for these cases are discussed below.

Table 2
Operating conditions and objective function (case 1) values corresponding to chromosomes A, B and C shown in Fig. 3a

Parameter	Chromosome A	Chromosome B	Chromosome C
F_{st} (kmol/h)	8.45	11.04	15.01
S_{st} (%)	94.86	92.69	87.51
T_{eb} (K)	651.53	713.52	799.98
P (bar)	1.84	1.84	2.03
SOR (−)	10.74	10.69	10.94
F^{o}_{eb} (kmol/h)	38.63	40.31	40.47
Y_{st} (%)	21.88	27.38	35.26
F_{bz} (kmol/h)	0.24	0.50	1.25
F_{tol} (kmol/h)	0.22	0.37	0.90
Profit ($ per h)	330	467	673

6.1. Case 1. Maximization of F_{st} and S_{st}

Fig. 3a shows the Pareto optimal set obtained after 100 generations with 50 chromosomes when the two objective functions considered are F_{st} and S_{st} (Eqs. (7) and (8)). The CPU time to generate the Pareto set was 45 s on a CRAY J916 supercomputer. Each point on the Pareto set corresponds to a set of decision variables given in Fig. 3b–e, where each of these decision variables is plotted against one of the Objectives, F_{st}. Fig. 3b–e reveal that optimum values for three of the decision variables (P, SOR and F^{o}_{eb}) are nearly constant and that the Pareto was due to conflicting effect of the decision variable (T_{eb}), which when increased increases F_{st} but decreases S_{st}. Table 2 compares objective functions (F_{st} and S_{st}), decision variables (T_{eb}, P, SOR and F^{o}_{eb}) and calculated values of Y_{st} for three selected chromosomes, A, B and C (shown in Fig. 3a). The conversion, temperature and pressure profiles for the three chromosomes (A, B and C) are shown in Fig. 4. Table 2 as well as Fig. 3a reveal that as we move from point A to point C, F_{st} increases while S_{st} decreases primarily due to increase of T_{eb} from 651.5 to 800 K. Fig. 3b shows that T_{eb} has a strong opposing effect on F_{st} and S_{st}. High T_{eb} maximizes styrene produced (F_{st}) while low T_{eb} maximizes styrene selectivity (S_{st}). This is due to the fact that the main reaction (Eq. (1)) is a reversible endothermic reaction. Temperature decreases along the length of the reactor, and, therefore, high temperature is required to achieve high conversion of ethyl benzene to styrene. This is shown in Fig. 4 where higher temperature profile for chromosome C results in higher values of Y_{st} (which is related to conversion) when compared with chromosome A. However, high temperature promotes thermal cracking leading to a decrease in the styrene selectivity. The optimal results also show that the decision variable, F^{o}_{eb} (Fig. 3e), hits the upper bound while moderately low SOR is chosen for optimal operation. It is obvious that high reactant flow rate will produce more styrene. High SOR is

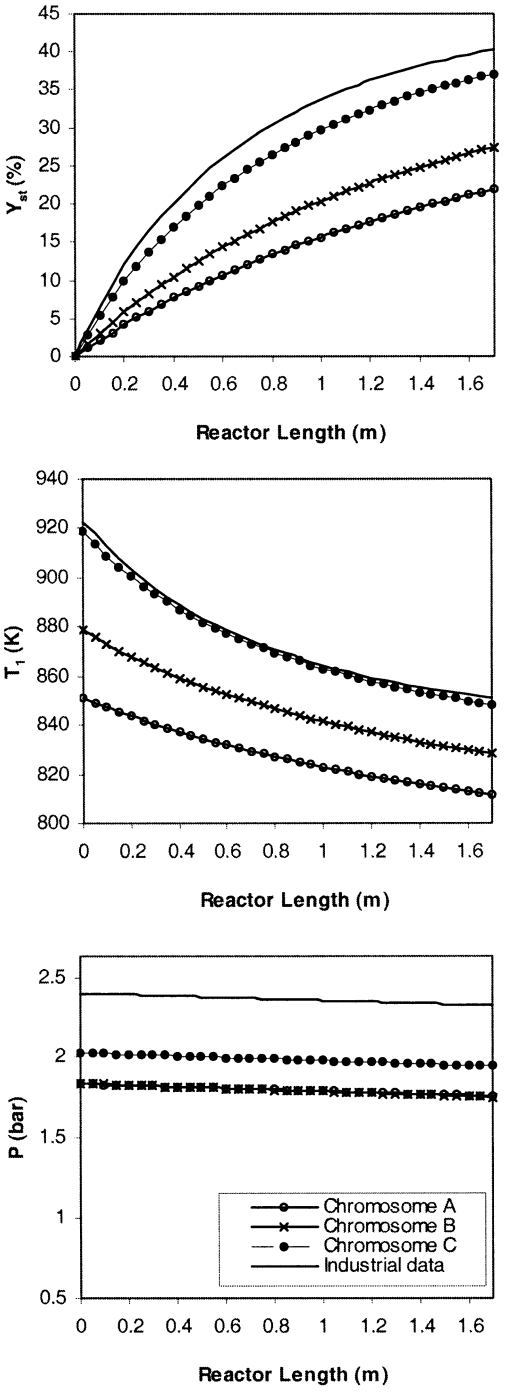

Fig. 4. Conversion, temperature and pressure profiles corresponding to chromosomes A, B and C and industrial operating point shown in Fig. 3a. (Case 1: maximization of F_{st} and S_{st}).

preferred for styrene operation as it shifts reaction 1 to the forward direction. However, the optimal SOR did not hit the upper bound as the constraint on total steam flow rate (= 454 kmol/h) restricted the optimal SOR value.

A profit function can be used as a guideline to select an operating point from the Pareto set. For this purpose, a simplified profit function is defined as:

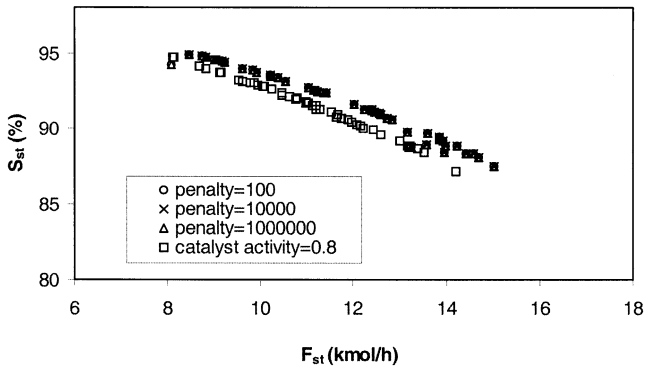

Fig. 5. Effect of the penalty coefficient in the objective functions (Eqs. (19)–(21)) and catalyst activity on the Pareto for the adiabatic reactor.

$$\text{Profit} = \text{Revenue by selling styrene and byproducts} - \text{ethyl benzene cost} - \text{steam cost}$$

$$= F_{st}H_{st} + F_{bz}H_{bz} + F_{tol}H_{tol} - [F^{o}_{eb} - F_{eb}]H_{eb} - F_{steam}H_{steam} \quad (27)$$

where, H_{st} is the cost of styrene (= \$103/kmol), H_{bz} is the cost of benzene (= \$30.8/kmol), H_{tol} is the cost of toluene (= \$33.9/kmol), H_{eb} is the cost of ethyl benzene (= \$45.6/kmol) and H_{steam} is the cost of superheated steam (= \$0.36/kmol). The price of styrene, ethyl benzene, benzene and toluene are based on recent (April 2001) published prices from on-line Purchasing magazine (http://www.purchasing.com). The above profit function and cost coefficients just serve as a guideline as these prices vary with time. Also, note that the profit function defined in Eq. (27) does not include operating cost (except cost of ethyl benzene and steam) such as separation costs involved in separation of by-products (benzene and toluene) from styrene and unconverted reactant.

Using the profit function in Eq. (27), profit for the three chromosomes is compared in Table 2. The maximum profit of \$673 per h is obtained for chromosome C for which F_{st} is 15.01 kmol/h and S_{st} is 87.51%. This is marginally better than industrial operating point (Sheel & Crowe, 1969; Elnashaie et al., 1993) shown by × in Fig. 3a. It can be seen that the industrial operating point (with $F_{st} = 14.9$ kmol/h, $S_{st} = 85.15\%$ and profit of \$651 per h) lies slightly below the Pareto. Hence, operating the styrene reactor corresponding to chromosome C, improves not only the profit by about 4% but also selectivity by more than 2%. Nevertheless, the Pareto obtained by the two-objective optimization (Fig. 3a) provides a set of optimal solutions and some of these are better if one wants to produce styrene with higher selectivity. High selective production will also reduce operating costs as cost of separation of by-products from styrene will be low, which has not been included in the profit function Eq. (27).

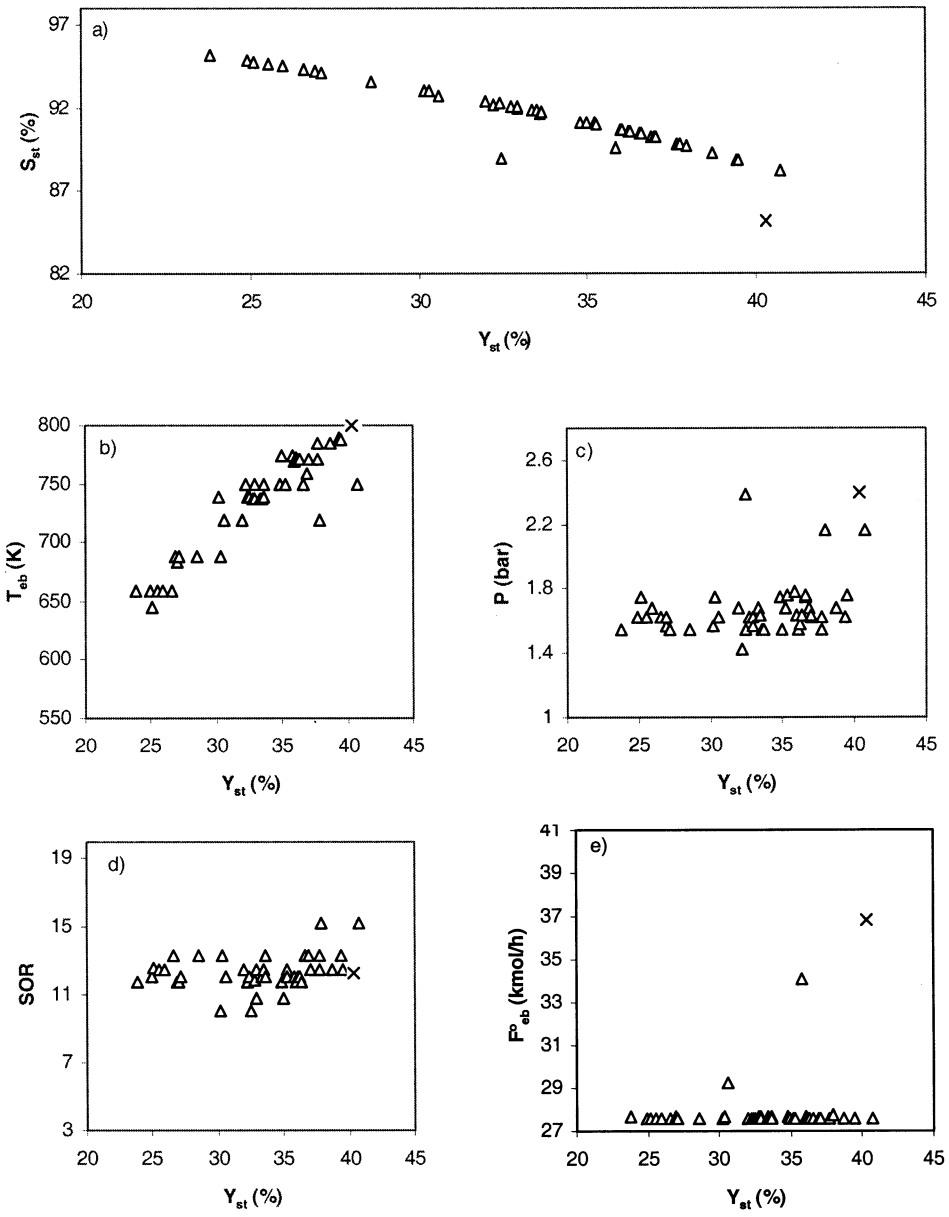

Fig. 6. Results for two-objective optimization (Case 2, maximization of S_{st} and Y_{st}). (a) Pareto set; and (b–e) values of decision variables corresponding to the points shown in (a), × indicates industrial operating point.

It can be seen from the results in Fig. 5 for three values of the penalty coefficient in Eqs. (19)–(21), that penalty value in the range considered has negligible effect on the Pareto. This is probably due to use of only objective function values (and not its derivatives) and a fitness function in GA. Fig. 5 also shows the effect of catalyst activity, which could deteriorate over a period of time. To simulate this, values of frequency factor (A_i) in Table A1 are multiplied by 0.8. This reduction in catalyst activity decreases optimal selectivity by about 1% for the same value of F_{st}.

6.2. Case 2. Maximization of S_{st} and Y_{st}

In this case, simultaneous maximization of S_{st} and Y_{st} (Eqs. (8) and (9)) is considered with the same set of decision variables with bounds (Eqs. (10)–(13)) and constraints (Eqs. (16)–(18)). Pareto and corresponding decision variables (Fig. 6a–e) reveal that once again T_{eb} has opposing effect on the objective functions while the other three decision variables are nearly constant. This is similar to the observation discussed earlier for case 1. However, optimal value of F^{o}_{eb} is at the lower bound in

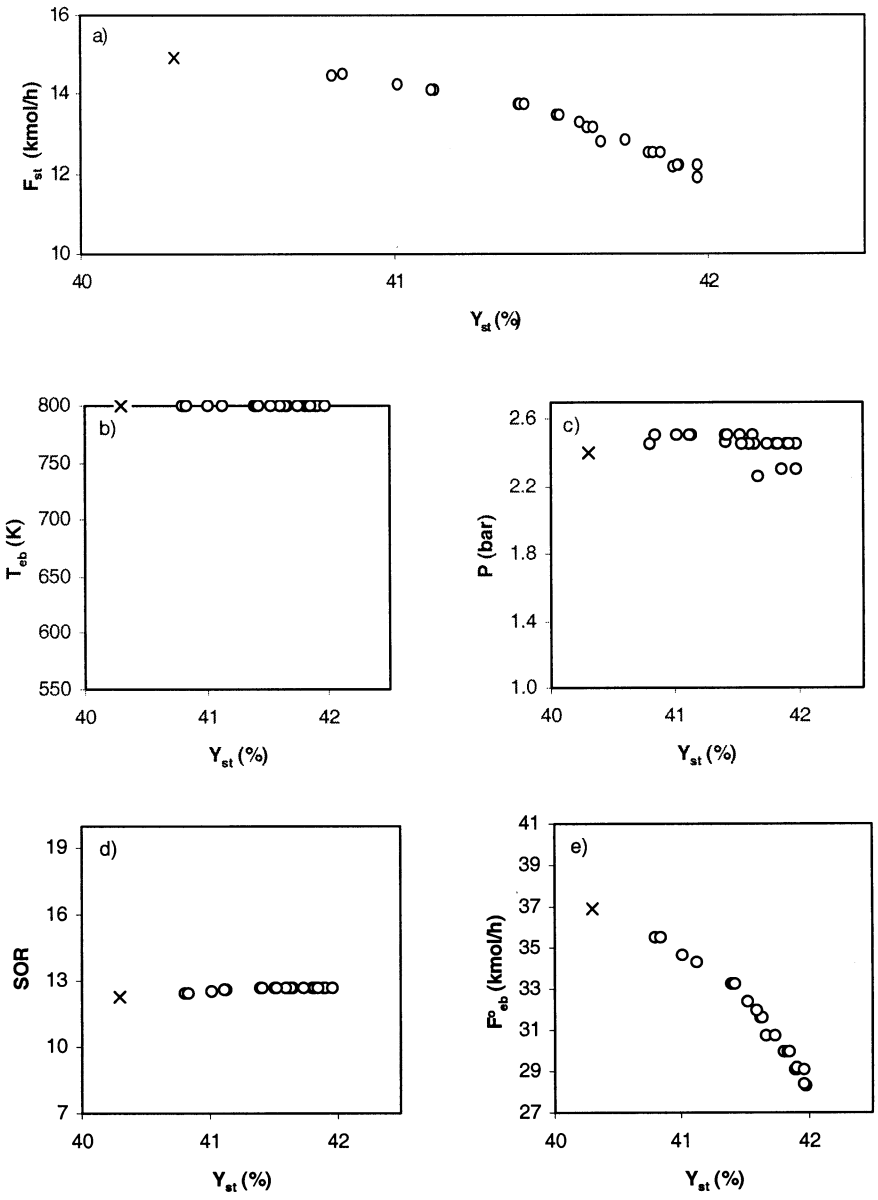

Fig. 7. Results for two-objective optimization (Case 3, maximization of F_{st} and Y_{st}). (a) Pareto set; and (b–e) values of decision variables corresponding to the points shown in (a), × indicates industrial operating point.

case 2 compared with case 1 where optimal F^{o}_{eb} was at the upper bound. This is expected as maximization of Y_{st}, is one of the objective functions in case 2, low reactant flow rate is selected to achieve higher styrene yield. Comparing the industrial data and the results obtained in case 2, it is found that the Pareto set obtained is better than the industrial operating point (Fig. 6a).

6.3. Case 3. Maximization of F_{st} and Y_{st}

Fig. 7a–e show the Pareto and corresponding decision variables when F_{st} and Y_{st} (Eqs. (7) and (9)) are maximized. This result is obtained using some of the GA parameters different from the other two cases (see Table 1). For case 1, high but constant F^{o}_{eb} was required to maximize F_{st} and S_{st}, while low but constant F^{o}_{eb} was required to maximize S_{st} and Y_{st} for case 2. When F_{st} and Y_{st} (case 3) were maximized simultaneously, F^{o}_{eb} found to be the controlling variable that resulted in non-dominated optimal solutions. The other three decision variables (T_{eb}, P and SOR) are practically constant. Fig. 7a further shows that the industrial point lies at one end of the Pareto, and it is perhaps one of the optimal solutions. However, the Pareto in Fig. 7a provides numerous optimal solutions (similar to Figs. 3a and

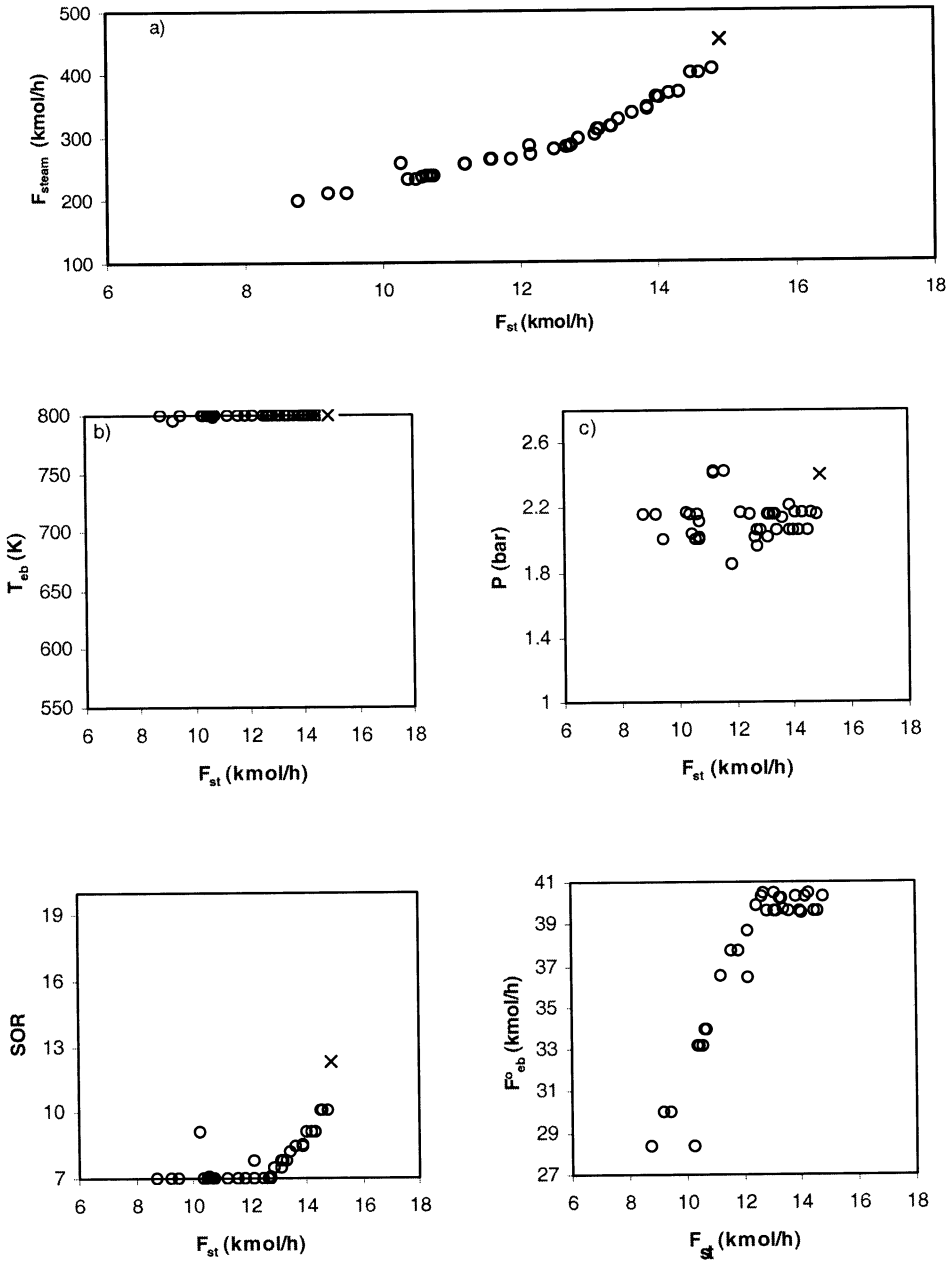

Fig. 8. Results for two-objective optimization (Case 3A, maximization of F_{st} and minimization of F_{steam}). (a) Pareto set at 100; (b–e) values of decision variables corresponding to the points shown in (a); × indicates industrial operating point.

6a), which are equally attractive and can provide a better solution if one likes to select an optimal point of high yield.

6.4. Case 3A. Maximization of F_{st} and minimization of F_{steam}

Since the profitability of styrene production is affected by the amount of steam used, another case to simultaneously maximize F_{st} and minimize flow rate of steam (F_{steam}) is studied. These results presented in Fig. 8, show that the Pareto in this case are due to the conflicting effect of SOR and F^{o}_{eb}. For minimizing F_{steam}, the process should employ less F^{o}_{eb} and less F_{steam} subject to the limits on SOR. On the other hand, maximizing F_{st} requires larger F^{o}_{eb} subject to the limits on both F^{o}_{eb} and SOR. The other two decision variables, T_{eb} and P are practically constant over the range of the Pareto, with the former at its upper bound (to reduce F_{steam}) and the latter at about 2.2 bars.

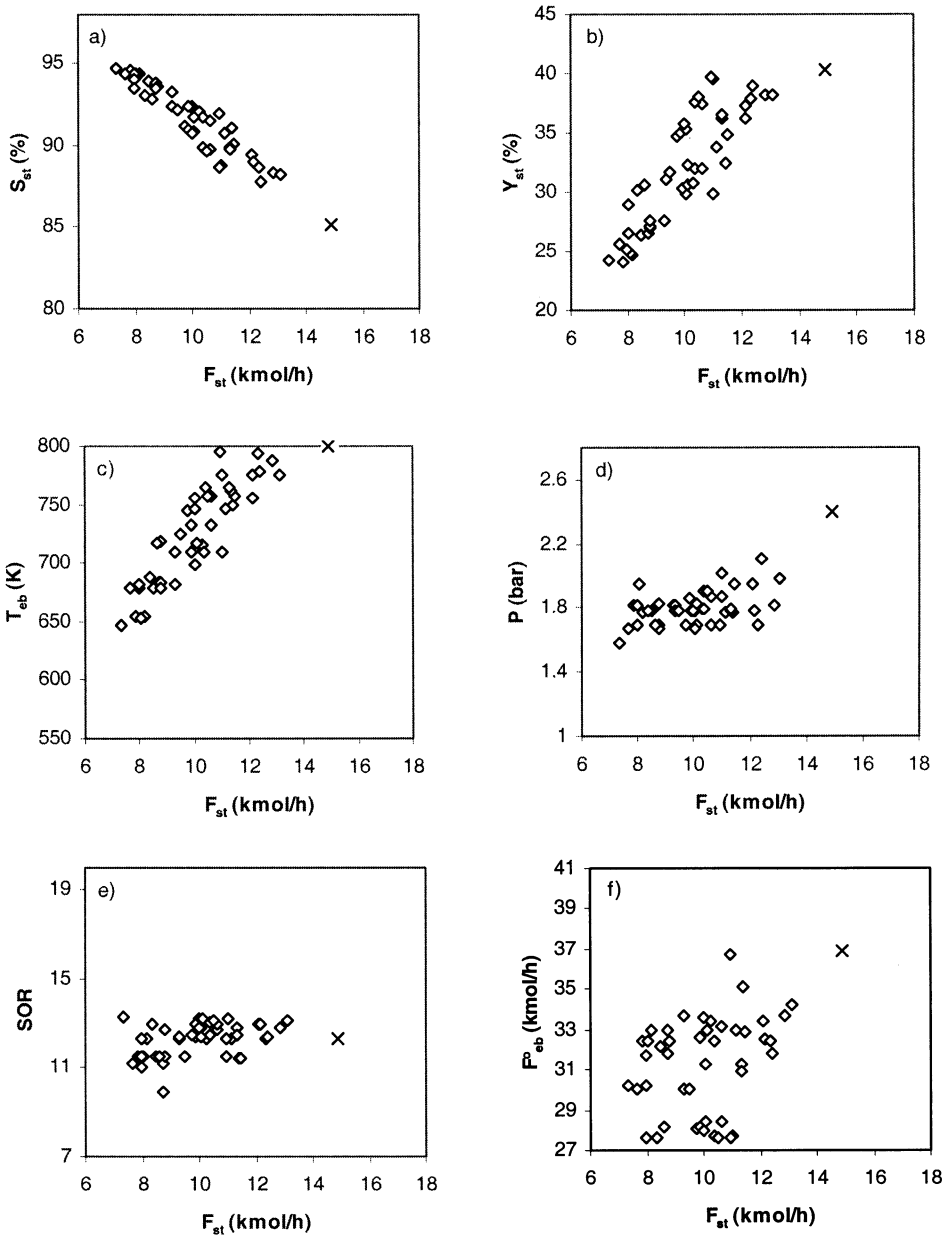

Fig. 9. Results for three-objective optimization (Case 4, maximization of F_{st}, S_{st} and Y_{st}). (a) and (b) Pareto set; and (c–f) values of decision variables corresponding to the points shown in (a) and (b); × indicates industrial operating point.

7. Three-objective optimization

More meaningful results can be expected if all three objectives (F_{st}, S_{st} and Y_{st}) are maximized simultaneously. When three-objective optimization (case 4) was performed using the same model for styrene reactor, the computation time required for obtaining the Pareto set was found to be the same as that for two-objective optimization cases, namely, 45 s on Cray J916 supercomputer for 50 chromosomes and 100 generations. The Pareto and corresponding decision variables from the three-objective optimization are presented in Fig. 9a–b and c–f, respectively. It can seen from Fig. 9a–b that, when one moves from one point to another in the Pareto set, both Y_{st} and F_{st} increases but S_{st} decreases. It was observed in two-objective function cases that Pareto was due to the conflicting effect of T_{eb} in cases 1 and 2, and F^{o}_{eb} in case 3. Fig. 9c shows that T_{eb} once again is the leading variable responsible in producing the Pareto for the 3-objective function case. Decision variable, F^{o}_{eb} is scattered with some trend of increasing with F_{st} (Fig. 9c). This is due to the opposing effect of F^{o}_{eb} on three objectives as seen in cases 1, 2 and 3 (Fig. 3e Fig. 6e Fig. 7e): high but constant F^{o}_{eb} is required to maximize F_{st} and S_{st} (case 1); low but constant F^{o}_{eb} is required to maximize S_{st} and Y_{st} (case 2); and F^{o}_{eb} is the controlling

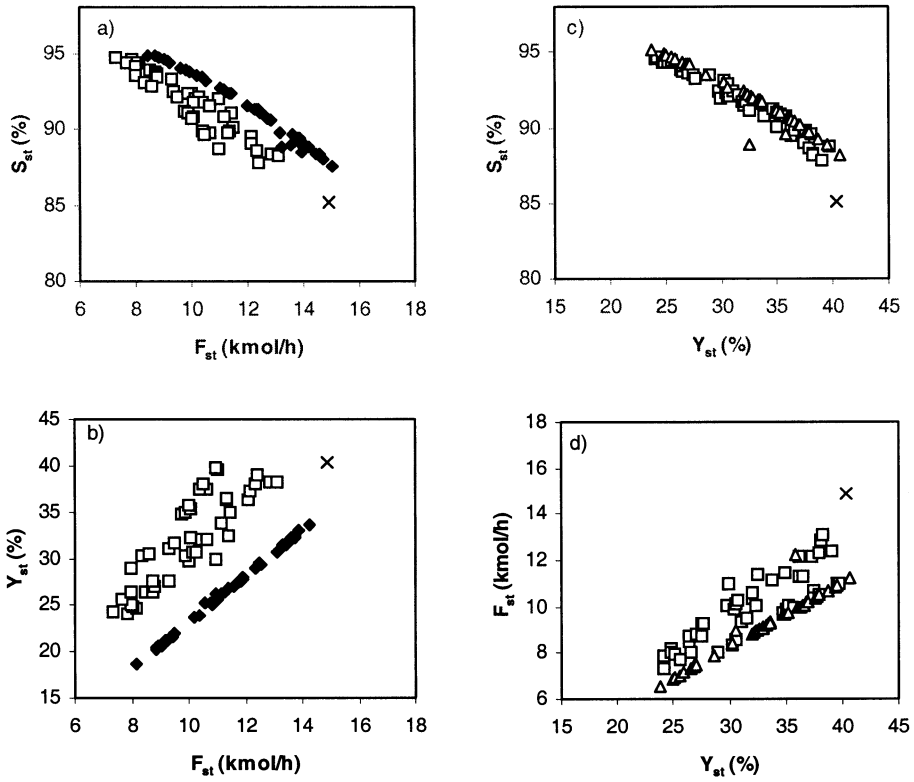

Fig. 10. Comparison of the Pareto set for three-objectives (Case 4 shown as □) with two-objectives (Case 1 shown as ◆ in (a) and (b), and Case 2 shown as △ in (c) and (d)); × indicates industrial operating point.

Table 3
Comparison of two-objective (case 1: maximization of F_{st} and S_{st}) and three-objective (case 4: maximization of F_{st}, S_{st} and Y_{st}) optimization results for a few selected values of F_{st} for the adiabatic reactor

F_{st} (kmol/h) (Objective 1)	Case 1		Case 4	
	S_{st} (%) (Objective 2)	Y_{st} (%) (Calculated)	S_{st} (%) (Objective 2)	Y_{st} (%) (Objective 3)
12.02	91.58	29.86	89.48	37.30
10.62	93.14	26.16	91.47	32.00
10.64	93.14	26.16	89.79	37.40
9.47	93.96	23.85	92.16	31.60

Table 4
Comparison of two-objective (case 2: maximization of S_{st} and Y_{st}) and three-objective (case 4: maximization of F_{st}, S_{st} and Y_{st}) optimization results for a few selected values of Y_{st} for the adiabatic reactor

Y_{st} (%) (Objective 1)	Case 2		Case 4	
	S_{st} (%) (Objective 2)	F_{st} (kmol/h) (Calculated)	S_{st} (%) (Objective 2)	F_{st} (kmol/h) (Objective 3)
38.03	89.70	10.54	88.30	12.85
32.26	92.20	8.89	91.77	10.08
32.49	92.20	8.89	91.08	11.40
25.65	94.65	7.04	94.37	7.68

variable responsible in yielding the Pareto in case 3. When three objective function optimization is performed, the effect of F_{eb}^{o} is cumulative, which results in the scatter of F_{eb}^{o} (Fig. 9e). Fig. 9a–b shows that the industrial point lies at one end of the Pareto and is perhaps one of the optimal solutions.

Fig. 10a–d show the comparison of the results for three-objective optimization and the two-objective cases

Table 5
Summary of the optimization results for adiabatic reactor

Parameter	Industrial	Case 1	Case 2	Case 3	Case 3A	Case 4
F_{st} (kmol/h)	14.90	15.01	10.89	14.48	14.79	13.09
S_{st} (%)	85.15	87.51	88.83	84.70	87.10	88.18
Y_{st} (%)	40.30	35.26	39.47	40.80	36.69	38.23
T_{eb} (K)	800.00	799.98	787.25	800.00	799.98	776.13
P (bar)	2.40	2.03	1.76	2.45	2.16	1.99
SOR (−)	12.29	10.94	12.54	12.47	10.10	13.16
F^{o}_{eb} (kmol/h)	36.87	40.47	27.58	35.49	40.31	34.24
F_{bz} (kmol/h)	1.37	1.25	0.85	1.36	1.13	1.10
F_{tol} (kmol/h)	1.20	0.90	0.52	1.25	1.06	0.66
Profit ($ per h)	651	673	482	637	673	565

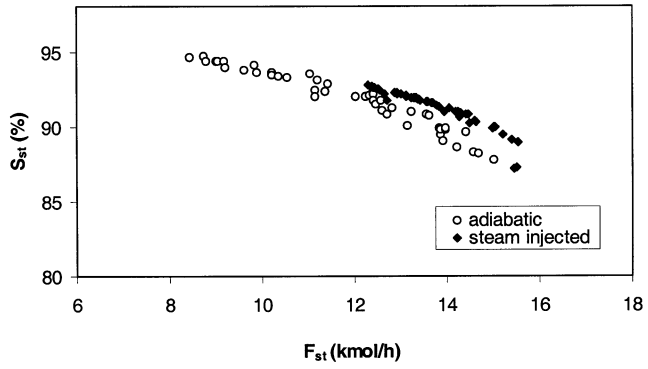

Fig. 11. Comparison of the Pareto set at $N_{gen} = 100$ for two-objective optimization (Case 1, maximization of F_{st}, and S_{st}) for adiabatic and steam-injected reactor.

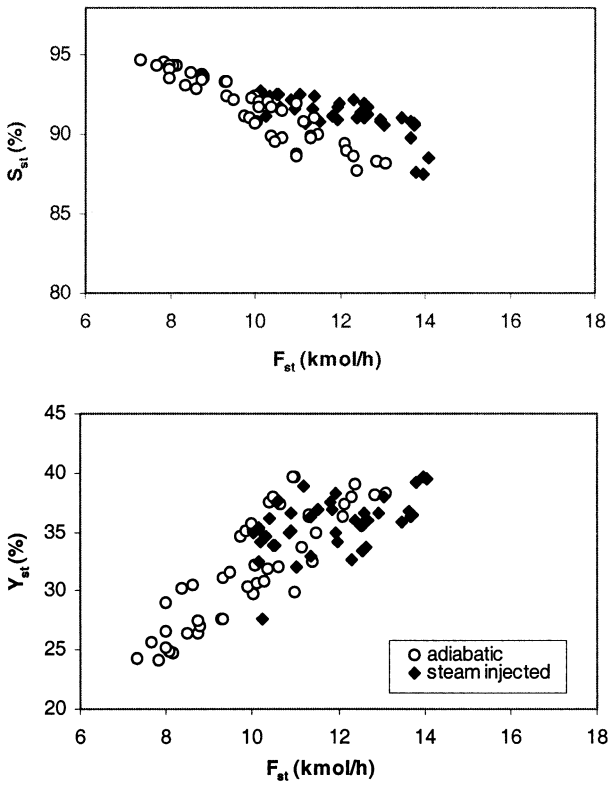

Fig. 12. Comparison of the Pareto at $N_{gen} = 100$ for three-objective optimization (Case 4, maximization of F_{st}, S_{st} and Y_{st}) for adiabatic and steam-injected reactor.

1 and 2. Tables 3 and 4 compare the results of two-objective cases (case 1 and case 2) with the three-objective case (case 4) for the same F_{st} (Table 3) and the same Y_{st} (Table 4) quantitatively. Fig. 10a–b and Table 3 show that for a fixed F_{st}, three-objective optimization results in a higher Y_{st} but marginally lower S_{st} than in case 1 of two-objective optimization. In addition, by comparing the two Pareto points having almost the same F_{st} (10.62 and 10.64 kmol/h) for the three-objective optimization, it is found that one of the points gives higher S_{st} (91.47%) but lower Y_{st} (32.00%) than another point (89.79, 37.40%). This is also observed in case 2 as shown in Table 4 for almost the same Y_{st} (32.26 and 32.49%), there is an improvement in F_{st} while S_{st} is lower.

A chromosome with the highest profit (Eq. (27)) is selected for each case of two-objective and three-objective optimization for the adiabatic reactor. The decision variables, objectives and profit corresponding to these selected chromosomes are shown in Table 5 along with those for the current industrial operating point. The profit for the industrial operating point is lower than case 1. However, it is higher in cases 2 and 3, and three-objective optimization (case 4). It is because profit strongly depends on F_{st} which is not one of the objectives in cases 2 and 3, and converged three-objective results do not include the region of industrial operating point (Fig. 9a–b). The profit for case 3A ($673 per h) is comparable to cases 1 and 3 as maximization of styrene produced is an objective function and there is an upper bound on the amount of steam used ($F_{steam} < 454$ kmol/h) in all of them.

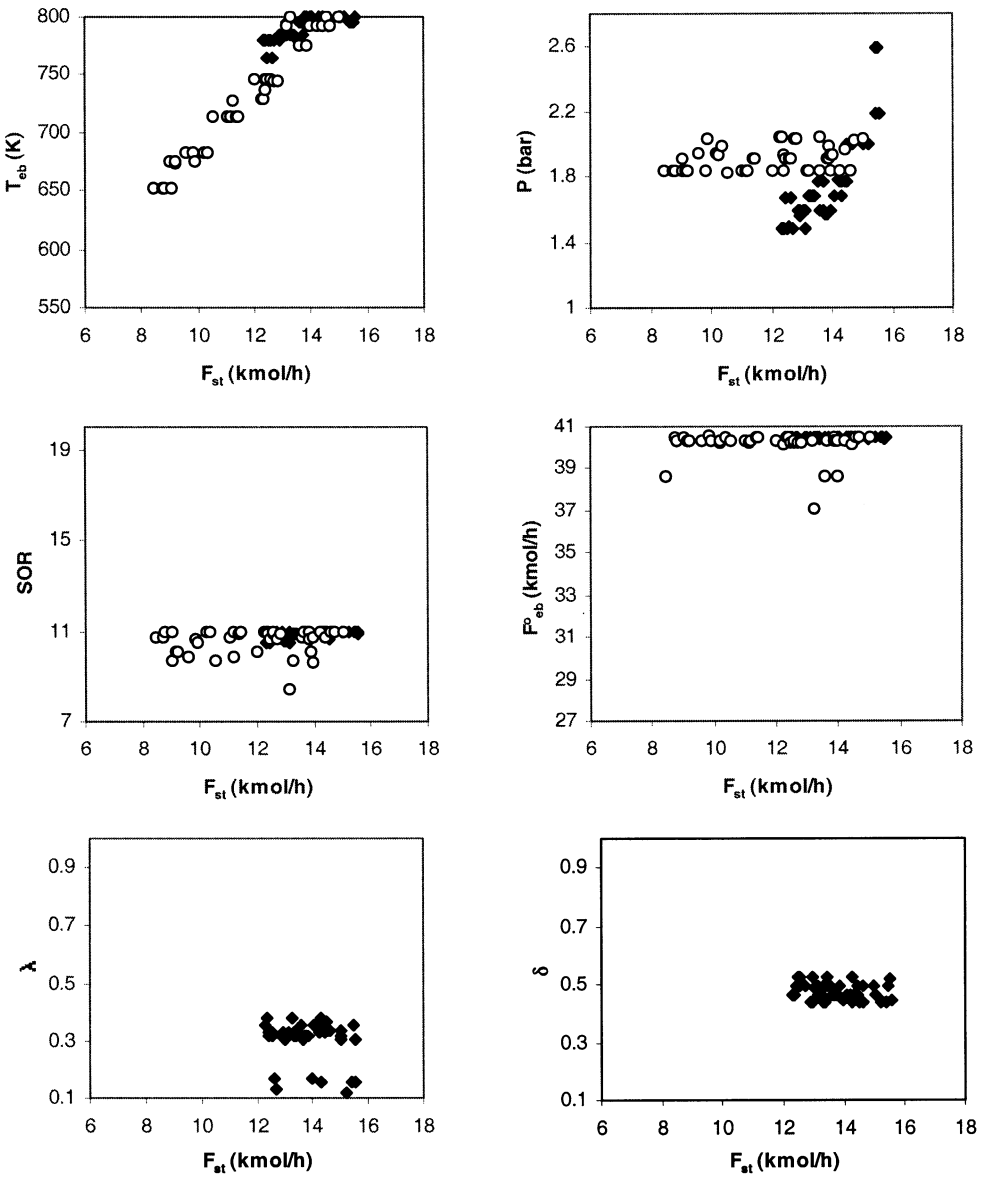

Fig. 13. Comparison of values of decision variables for adiabatic (○) and steam-injected reactor (◆) corresponding to the points on the Pareto set in Fig. 11.

8. Steam-injected reactor

Optimization problem of the industrial reactor assuming some steam injection at a point along the length of the reactor, is now studied. In this reactor configuration (Fig. 2), the total steam is divided into two portions: one part (δF_{steam}) is introduced at the reactor inlet while the remaining portion $[(1-\delta)F_{\text{steam}}]$ is injected at some location along the reactor length ($z=\lambda L$) to achieve the pseudo-isothermal condition. The optimization problem solved is the same as before (Eqs. (7)–(13), (16) and (17)) except for two additional decision variables (Eqs. (14) and (15)), namely, fraction of steam used at the reactor inlet (δ) and location at which the steam is injected (λ). Only results for case 1 of two-objective optimization and three-objective (case 4) optimization are discussed in detail. The CPU time taken to obtain one Pareto set for 100 generations and 50 chromosomes is 159 s on Cray J916 supercomputer.

Figs. 11 and 12 show the comparison of Pareto set obtained for adiabatic and steam-injected reactor, for case 1 and three-objective optimization, respectively. These figures reveal that splitting steam into two parts gives better optimal results at higher F_{st}. Low F_{st} is not possible to obtain as it tends to violate the constraint on T_1 (Eq. (17)). Figs. 13 and 14 show the plot of six decision variables corresponding to each point on the Pareto for two-objective (case 1, Fig. 11) and three-objective (case 4, Fig. 12) optimization, respectively. It is observed that the effect of four decision variables (T_{eb},

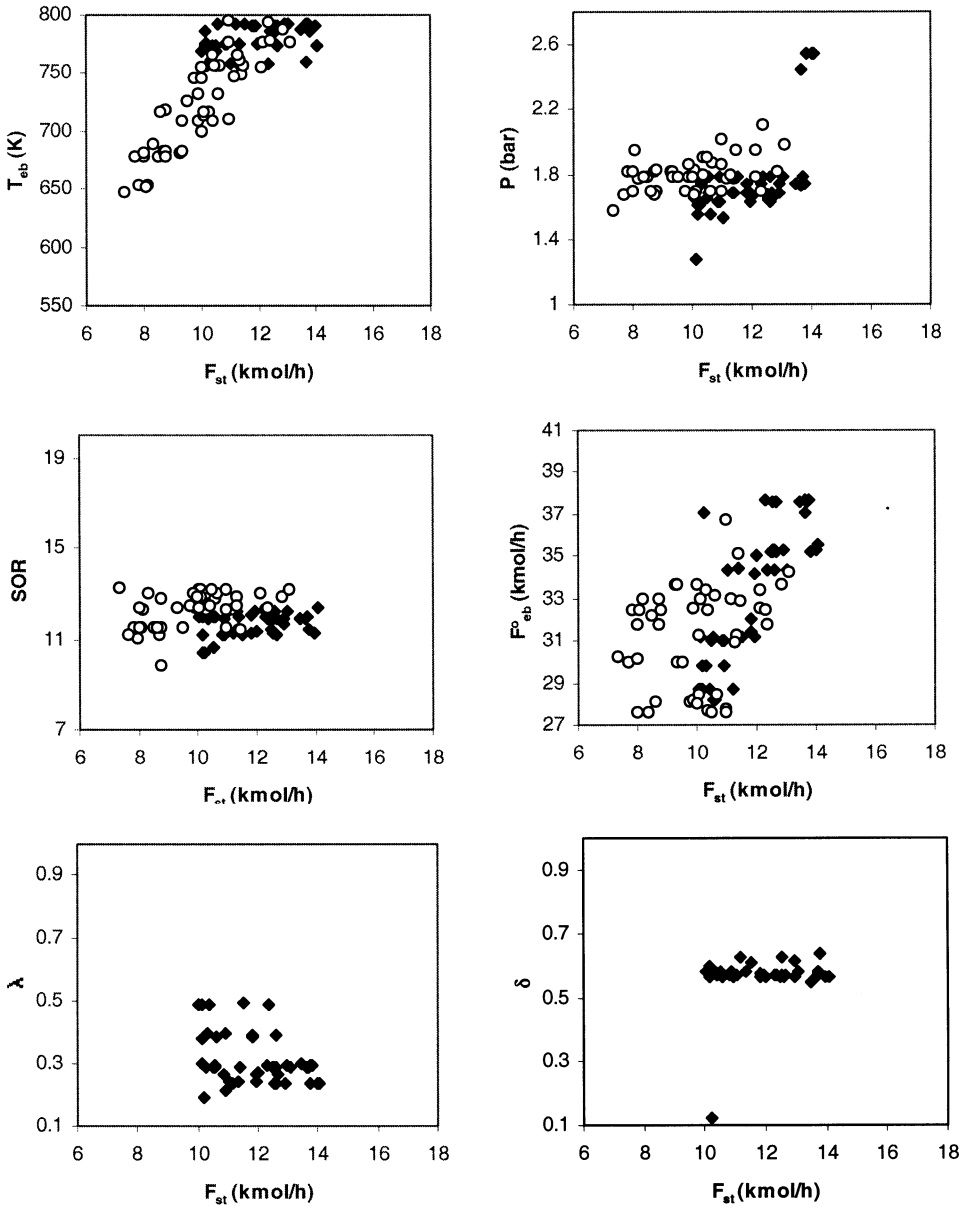

Fig. 14. Comparison of values of decision variables for adiabatic (○) and steam-injected reactor (◆) corresponding to the points on the Pareto set in Fig. 12.

P, SOR and F^{o}_{eb}) is similar to that obtained for the adiabatic reactor. Low T_{eb} leads to T_1 less than 850 K (allowable lower bound, Eq. (17)) due to the diversion of some steam for later injection (at $z = \lambda L$), and, therefore, violates the constraints on F_{steam} and T_1 (Eqs. (16) and (17)). Hence, the optimal T_{eb} selected for steam injection reactor is not as low as that of the adiabatic reactor. Fig. 15 compares temperature and pressure profiles for adiabatic and steam injection reactor for two objective optimization (case 1) at the same F_{st} value of 15.01 kmol/h. This figure shows that the temperature in the case of steam injection drops drastically at approximately 30% of the reactor length, which decreases Y_{st}. Thus, temperature must be brought up at this section to achieve higher Y_{st}. The decision variable plots (Fig. 13) show that the optimal location of steam injection is about 30% of the reactor length and that the optimal value of steam split is about 50%. If less steam is injected into the reactor inlet, T_1 will be low slowing reaction 1, which will lower Y_{st}. It is also observed in Fig. 4 that Y_{st} increases drastically with high inlet temperature, and thus it will not be advantageous to inject less steam at the reactor inlet. However, if large amount of steam is injected at the reactor inlet, T_2 obtained will be lower. The optimal value of about 50% split of total steam, therefore, ensures moderately high T_1 and T_2.

Results for the chromosome with highest profit in cases 1 to 4 are summarized in Table 6, which shows that

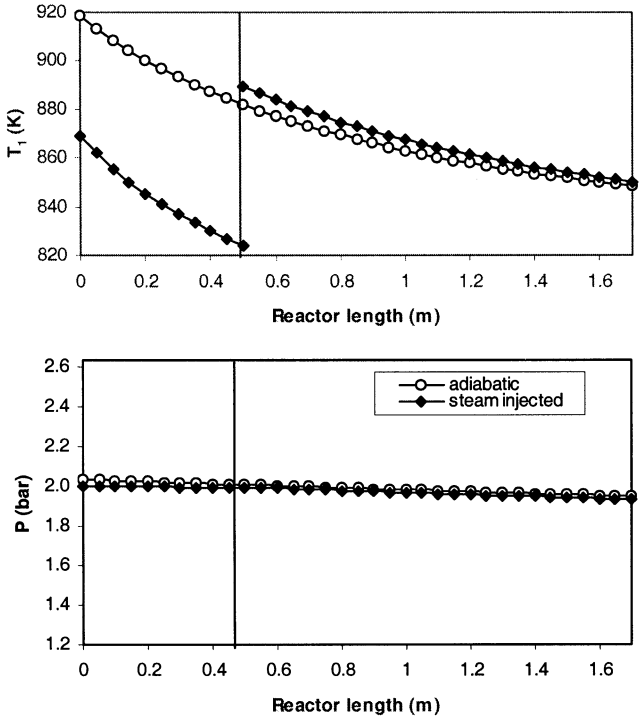

Fig. 15. Temperature and pressure profile for two-objective optimization (Case 1, maximization of F_{st} and S_{st}) for both adiabatic and steam-injected reactor at the same F_{st} of 15.01 kmol/h.

Table 6
Summary of the optimization results for steam injected reactor

Parameter	Case 1	Case 2	Case 3	Case 4
F_{st} (kmol/h)	15.51	12.56	15.97	13.97
S_{st} (%)	87.26	88.70	85.00	87.50
Y_{st} (%)	38.43	45.21	39.64	39.62
T_{eb} (K)	795.08	799.91	800.00	791.41
P (bar)	2.59	2.10	2.63	2.54
SOR (−)	10.89	15.53	11.06	11.30
F^{o}_{eb} (kmol/h)	40.36	27.78	40.29	35.27
λ (−)	0.30	0.33	0.11	0.24
δ (−)	0.52	0.47	0.97	0.57
F_{bz} (kmol/h)	0.81	0.83	0.95	0.77
F_{tol} (kmol/h)	1.45	0.77	0.99	1.23
Profit ($ per h)	703	544	723	633

the profit calculated based on Eq. (27) for steam-injected reactor is better than the corresponding value in Table 5 for adiabatic reactor, by 4–12%. This improvement is primarily due to the increase in the amount of styrene produced, and less by-products formation. Comparing the objective function values (F_{st}, Y_{st} and/or S_{st}) in Tables 5 and 6, it is observed that steam-injected reactor generally gives higher values of the objective functions than the adiabatic reactor.

The comparison of the results of steam injected reactor for three-objective function and the two-objective function (case 1) are shown in Table 7 for selected chromosomes. These are similar to those for the adiabatic reactor in Table 3.

9. Conclusions

Several multiobjective optimization problems for both adiabatic and steam-injected styrene reactors were formulated, and then solved by NSGA. Pareto optimal sets were successfully obtained for all situations considered The Pareto set and optimal operating conditions for different combinations of two objectives, are different. The trend of decision variables at the optimum in all cases can be explained qualitatively, which shows that the multiobjective optimization results obtained by NSGA are reliable. The results of multiobjective optimization shows that objectives such as production rate, selectivity and yield besides profit can be improved compared with the current operating condition. As expected, steam injection is better than adiabatic operation. The optimal results obtained are, in general, valuable for engineer to study and understand the reactor operation, and in choosing the best operating conditions to satisfy specified objectives. Although NSGA has been reasonably successful for multi-objective optimization, our experience shows that suitable values for its parameters will have to be selected through several trials and that it often gives near optimal solutions. Hence, NSGA requires further improvements

Table 7
Comparison of two-objective (case 1: maximization of F_{st} and S_{st}) and three-objective (case 4: maximization of F_{st}, S_{st} and Y_{st}) optimization results for a few selected values of F_{st} for the steam injected reactor

F_{st} (kmol/h) (Objective 1)	Case 1		Case 4	
	S_{st} (%) (Objective 2)	Y_{st} (%) (Calculated)	S_{st} (%) (Objective 2)	Y_{st} (%) (Objective 3)
12.32	92.75	30.40	92.19	32.67
13.73	91.55	33.84	90.63	36.50
13.74	91.55	33.84	90.68	36.44
14.06	91.20	34.74	88.53	39.54

for obtaining optimal solutions of multi-objective problems accurately and reliably.

Appendix A: Model, design and operating conditions for a styrene reactor

The governing equations for the pseudo-homogeneous model, which was used for the multiobjective optimization, are given below (Sheel & Crowe, 1969; Elnashaie & Elshishini, 1994).

Mass balance:

$$\frac{dX_i}{dz} = \frac{\rho_b A_t r_i}{F_{eb}^o} \quad (A1)$$

where, X_i is the fractional conversion of ethyl benzene in each of the three reactions, $i = 1$, 2 and 3. For the other three reactions, $i = 4$, 5 and 6, X_i is given by:

$$\frac{dX_i}{dz} = \frac{\rho_b A_t r_i}{F_{steam}^o} \quad (A2)$$

Energy balance:

$$\frac{dT}{dz} = \frac{\sum_{i=1}^{6}(-\Delta H_i)\rho_b A_t r_i}{\sum_j F_j Cp_j} \quad (A3)$$

Pressure drop along the reactor length is given by Ergun equation:

$$\frac{dP}{dz} = 1 \times 10^{-5}\frac{(1-\varepsilon)G_o}{D_p \varepsilon^3 \rho_G}\left[\frac{150(1-\varepsilon)\mu_G}{D_p} + 1.75G_o\right] \quad (A4)$$

Rate expression and kinetic data for the six reactions are summarized in Table A1, while the design and operating conditions for an industrial reactor are shown in Table A2. The predicted results by the model are compared with the industrial data in Table A3.

Table A1
Rate expression and data for the six reactions (Elnashaie & Elshishini, 1994)

Reaction expression	E_i (kJ/kmol)	A_i
$r_1 = k_1(p_{eb} - p_{st}p_{H_2}/K_{eb})$	90 981.4	−0.0854
$r_2 = k_2 p_{eb}$	207 989.2	13.2392
$r_3 = k_3 p_{eb} p_{H_2}$	915 15.3	0.2961
$r_4 = k_4 p_{steam} p_{eth}^{0.5}$	103 996.7	−0.0724
$r_5 = k_5 p_{steam} p_{meth}$	65 723.3	−2.9344
$r_6 = k_6(P/T^3)p_{steam}p_{CO}$	73 628.4	21.2402

[2] Notes: k_i (kmol/kg per s per bar^n) = exp($A_i - E_i/RT$); p refers to partial pressure of the reactant given in the subscript; equilibrium constant, K_{eb} for reaction 1 is given by exp[−(122 725 − 126.3 T − 0.002194 T^2)/8.314 T].

Table A2
Design and operating conditions for the industrial reactor (Sheel & Crowe, 1969; Elnashaie & Elshishini, 1994).

Quantity	Numerical value
Reactor diameter	1.95 m
Reactor length/catalyst bed depth	1.7 m
Catalyst bulk density	2146 kg/m^3
Catalyst particle diameter	0.0047 m
Bed void fraction	0.445
Catalyst composition	62% Fe_2O_3, 36% K_2CO_3, 2% Cr_2O_3
Inlet pressure	2.4 bar
Inlet temperature	922.59 K
Ethyl benzene in the feed	36.87 kmol/h
Styrene in the feed*	0.67 kmol/h
Benzene in the feed*	0.11 kmol/h
Toluene in the feed*	0.88 kmol/h
Steam	453.1 kmol/h

[3] These three components are present as impurities in the ethyl benzene feed shown in Fig. 2.

Table A3
Comparison of the simulation results with the industrial data (Sheel & Crowe, 1969; Elnashaie & Elshishini, 1994).

Quantity at reactor exit	Industrial data	Simulation results
Exit temperature (K)	850.0	849.75
Exit pressure (bar)	2.32	2.33
Ethyl benzene conversion (%)	47.25	46.74
Ethyl benzene flow rate (kmol/h)	19.45	19.63
Styrene flow rate (kmol/h)	15.57	15.40
Benzene flow rate (kmol/h)	1.5	1.44
Toluene flow rate (kmol/h)	2.03	2.05

Appendix B: Genetic algorithm (GA) and NSGA

GA is a search technique developed by Holland (1975). This method mimics the principles of natural evolution. For this technique, the set of decision variables is first decoded string structures in binary numbers (0 and 1). These are known as 'chromosomes' and hence create a population (gene pool). Each of these chromosomes is then mapped into its real value using lower and upper bounds specified for the decision variables. A model of the process will then compute an objective function for each chromosome and these functions reflect the 'fitness' of the chromosome.

The optimization search proceeds through three operations: reproduction, crossover and mutation. The reproduction operation selects good strings in a population and forms a mating pool. The chromosomes are copied based on their fitness value. No new strings are produced in this operation. The crossover allows for a

new string formation by exchanging some portion of the string (chosen randomly) with the string of another chromosome generating daughter chromosomes in the mating pool. If the daughter chromosomes are less fit than parent chromosomes, they will slowly die natural death in the subsequent generation. The effect of crossover can be detrimental or good. Hence, not all strings are used for crossover. A crossover probability, P_c is used, where only 100 P_c percent of the strings in the mating pool are involved in crossover while the rest continue unchanged to the next generation. The last operation is mutation. This operation changes 1 to 0 and vice versa using a small mutation probability P_m. The mutation alters a string locally to create a better string. Mutation is needed to create a point in the neighborhood of the current point, thereby achieving a local search around the current solution and to maintain diversity in the population. The entire process is repeated till some termination criterion is met (the specified maximum number of generations is attained, or the improvements in the values of the objective functions become lower than a specified tolerance). A detailed description of GA is documented in Holland (1975) and Goldberg (1989).

The optimal solution to a multipleobjective function results in Pareto optimal set rather than unique solution. A Pareto set is such that when one moves from one point to another on the Pareto, one objective function improves while the other worsens. Neither of the solutions dominates over each other and all the sets of decision variables on the Pareto are equally good. Hence, the simple genetic algorithm is modified to a new algorithm known as NSGA to obtain Pareto solution. This new algorithm differs by the way the operators are selected.

NSGA uses a ranking method to emphasize the good points and a niche method to create diversity in the population without losing a stable sub-population of good points. In the new procedure, several groups of chromosomes at any generation are identified and classified into fronts. Each of the members in a particular front is assigned a large, common, front fitness value (a dummy value) arbitrarily. The dummy fitness value is then modified according to a sharing procedure. The points in this (or any other) front are then distributed evenly in the decision variable domain by dividing it by the niche count of the chromosome. The niche count is a quantity that represents the number of neighbors around it. The niche count gives an idea of how crowded the chromosomes are in the decision variable space. This helps spread out the chromosomes in the front since crowded chromosomes are assigned lower fitness values. This procedure is repeated for all the members of the first front. These chromosomes are then temporarily removed from consideration. All the remaining ones are tested for non-dominance. The non-dominated chromosomes in this round are classified into the next front. These are all assigned a dummy fitness value that is slightly lower than the lowest shared fitness value of the previous front. Sharing is performed thereafter. The sorting and sharing is continued till all the chromosomes in the gene pool are assigned shared fitness values. The usual operations of reproduction, crossover and mutation are now performed. Non-dominated members of the first front that have fewer neighbors, will get the highest representation in the mating pool while dominated members of later fronts will get lower representations (they are still assigned some low fitness values, rather than 'killed', in order to maintain the diversity of the gene pool). Sharing forces the chromosomes to be spread out in the decision variable space. It is to be noted that any number of objectives (both minimization and maximization problems) can be solved using this procedure. Hence, the method searches for a better set of operating conditions for multi-objective optimization. Additional details about the algorithm, its comparison over other techniques and some comments on the choice of the computational parameters to be used in NSGA, are described elsewhere (Srinivas & Deb, 1995; Deb, 2001).

References

Abdalla, B. K., Elnashaie, S. S. E. H., Alkhowaiter, S., & Elshishini, S. S. (1994). Intrinsic kinetics and industrial reactors modeling for the dehydrogenation of ethyl benzene to styrene on promoted iron oxide catalysts. *Applied Catalysis A: General 113*, 89–102.

Bhaskar, V., Gupta, S. K., & Ray, A. K. (2000). Application of multi-objective optimization in chemical engineering. *Reviews in Chemical Engineering 16* (1), 1–54.

Box, M. J. (1965). A new method of constrained optimization and a comparison with other methods. *Computer Journal 8*, 42.

Chen, S. S. (1992). Styrene. In J. I. Kroschwitz & H. G. Mary (Eds.), *Encyclopedia of chemical technology*, vol. 22 (pp. 956–994). New York: Wiley.

Clough, D. E., & Ramirez, W. F. (1976). Mathematical modeling and optimization of the dehydrogenation of ethyl benzene to form styrene. *American Institute of Chemical Engineering Journal 22*, 1097–1105.

Deb, K. (2001). *Multi-objective optimization using evolutionary algorithms*. New York: Wiley.

Denis, H. J., & Castor, W. M. (1992). Styrene. In B. Elvers, S. Hawkin & W. Russey (Eds.), *Ullmann's encyclopedia of industrial chemistry*, vol. A25 (pp. 325–335). New York: Wiley.

Elnashaie, S. S. E. H., Abdalla, B. K., & Hughes, R. (1993). Simulation of the industrial fixed bed catalytic reactor for the dehydrogenation of ethyl benzene to styrene: heterogeneous dusty gas model. *Industrial and Engineering Chemistry Research 32*, 2537–2541.

Elnashaie, S. S. E. H., & Elshishini, S. S. (1994). *Modelling, simulation and optimization of industrial fixed bed catalytic reactors*. London: Gordon and Breach Science Publisher.

Li, C. H., & Hubbell, O. S. (1982). Styrene. In J. J. Mcketta & G. E. Weismantel (Eds.), *Encyclopedia of chemical processing and design*, vol. 55 (pp. 197–217). New York: Wiley.

Rajesh, J., Gupta, S. K., Rangaiah, G. P., & Ray, A. K. (2000). Multiobjective optimization of steam reformer using genetic algorithm. *Industrial and Engineering Chemistry Research 39* (3), 706–717.

Rajesh, J., Gupta, S. K., Rangaiah, G. P., & Ray, A. K. (2001). Multiobjective optimization of industrial hydrogen plants. *Chemical Engineering Science 56* (3), 999–1010.

Savoretti, A. A., Borio, D. O., Bucalá, V., & Porras, J. A. (1999). Non-adiabatic radial-flow reactor for styrene production. *Chemical Engineering Science 54*, 205–213.

Sheel, J. G. P., & Crowe, C. M. (1969). Simulation and optimization of an existing ethyl benzene dehydrogenation reactor. *Canadian Journal of Chemical Engineering 47*, 183–187.

Sheppard, C. M., Maier, E. E., & Caram, H. S. (1986). Ethyl benzene dehydrogenation reactor model. *Industrial and Engineering Chemical Process Design Development 25*, 207–210.

Srinivas, N., & Deb, K. (1995). Multiobjective function optimization using nondominated sorting genetic algorithms. *Evolutionary Computation 2*, 221–248.

Sundaram, K. M., Sardina, H., Fernandez-Baujin, J. M., & Hildreth, J. M. (1991). Styrene plant simulation and optimization. *Hydrocarbon Processing 70*, 93–97.

Wenner, R. R., & Dybdal, E. C. (1948). Catalytic dehydrogenation of ethyl benzene. *Chemical Engineering Progress 44*, 275–286.